

Deeper but smaller: Higher-order interactions increase linear stability but shrink basins

Yuanzhao Zhang,^{1,*} Per Sebastian Skardal,² Federico Battiston,³ Giovanni Petri,^{4,5,6} and Maxime Lucas^{5,†}

¹*Santa Fe Institute, Santa Fe, NM, USA*

²*Department of Mathematics, Trinity College, Hartford, CT 06106, USA*

³*Department of Network and Data Science, Central European University, 1100 Vienna, Austria*

⁴*NP Lab, Network Science Institute, Northeastern University London, London, UK*

⁵*CENTAI Institute, 10138 Torino, Italy*

⁶*IMT Lucca, Lucca, Italy*

A key challenge of nonlinear dynamics and network science is to understand how higher-order interactions influence collective dynamics. Although many studies have approached this question through linear stability analysis, less is known about how higher-order interactions shape the global organization of different states. Here, we shed light on this issue by analyzing the rich patterns supported by identical Kuramoto oscillators on hypergraphs. We show that higher-order interactions can have opposite effects on linear stability and basin stability: they stabilize twisted states (including full synchrony) by improving their linear stability, but also make them hard to find by dramatically reducing their basin size. Our results highlight the importance of understanding higher-order interactions from both local and global perspectives.

I. INTRODUCTION

Higher-order interactions [1–6] connecting more than two units simultaneously are key in shaping complex dynamical processes such as contagion and evolution in social networks [7–12], information processing in the brain [13–16], and synchronization in coupled oscillators [17–21]. Understanding how they influence collective dynamics is thus essential. A variety of studies have approached this challenge from a linear stability perspective, which characterizes how states such as synchronization and consensus respond to small perturbations [22–33]. However, little attention has been paid to basin stability [34], a global measure based on the size of basins of attraction, which dictates the system’s response to large perturbations [35–39].

In this paper, we provide a more complete picture of how higher-order interactions influence dynamical patterns, in terms of both linear and basin stability. We show that higher-order interactions can have opposite effects: they can create more sync states by making them linearly stable; at the same time, higher-order interactions also dramatically shrink their attraction basins, effectively hiding them. As a result, states such as full synchrony may be stable but unreachable from random initial conditions.

To demonstrate this point, we consider n identical phase oscillators coupled through both pairwise and tri-

adic interactions:

$$\begin{aligned} \dot{\theta}_i = \omega + \frac{\sigma}{k_i^{(1)}} \sum_{j=1}^n A_{ij} \sin(\theta_j - \theta_i) \\ + \frac{\sigma_{\Delta}}{2k_i^{(2)}} \sum_{j,k=1}^n B_{ijk} \sin(\theta_j + \theta_k - 2\theta_i). \end{aligned} \quad (1)$$

Equation (1) is a generalization of the Kuramoto model [40] and emerges naturally from the higher-order phase reduction of limit-cycle oscillators [17]. Here, $\theta_i \in S^1$ represents the phase of oscillator i and ω is their common frequency. The adjacency tensors determine which oscillators interact: $A_{ij} = 1$ if nodes i and j have a pairwise connection, and zero otherwise. Similarly, $B_{ijk} = 1$ if and only if nodes i , j , and k are coupled through a triadic interaction. The coupling strengths are given by σ and σ_{Δ} , respectively, and are normalized by $k_i^{(\ell)}$, the ℓ th order degree of node i .

The case of pairwise coupling ($\sigma_{\Delta} = 0$) has been studied in detail from both linear and basin stability perspectives. While full synchrony $\theta_i(t) = \theta_j(t) \forall i, j, t$ is always an attractor of Eq. (1), additional attractors can emerge but only when networks are not too dense [41–44]. For ring networks, these attractors are *twisted states* and they emerge for link density below 0.68 [45]. In a q -twisted state $\theta^{(q)}$, the phases make q full twists around the ring and satisfy $\theta_k^{(q)} = 2\pi kq/n + C$, where q is the *winding number* [c.f. Fig. 1(a)]. In particular, the fully synchronized state corresponds to $q = 0$. For rings with nearest-neighbor couplings, the number of attractors grows linearly with n , since twisted states with up to $n/4$ twists are stable [46, 47]. A fruitful line of research aims to characterize the basins of the coexisting twisted states, which has revealed interesting scaling relations between basin size and winding number [45, 48, 49] as well as tentacle-like structures in the basins [49–51].

* yzhang@santafe.edu

† maxime.lucas@centai.eu

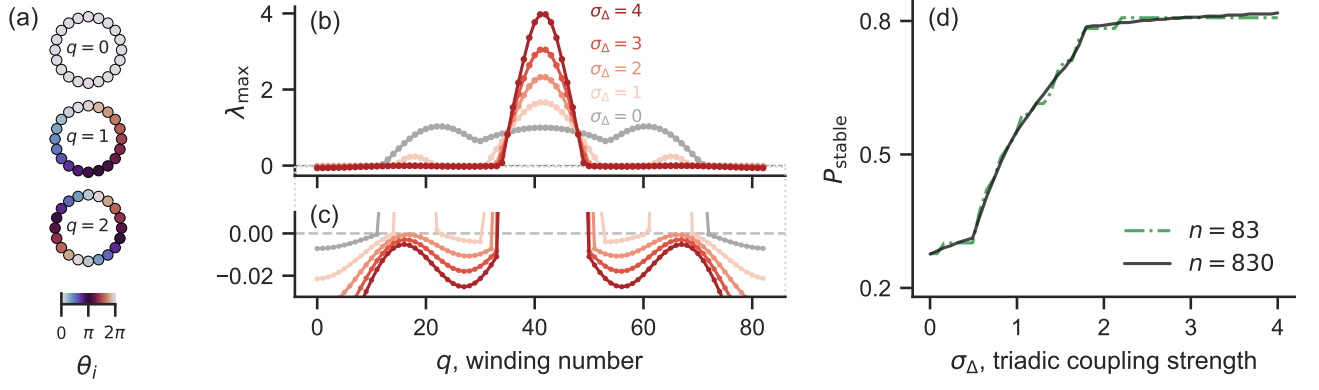


FIG. 1. **Higher-order interactions improve the linear stability of twisted states.** (a) Example twisted states with different winding numbers, for $n = 20$. Full synchrony corresponds to $q = 0$. (b) Linear stability (measured by the largest transverse Lyapunov exponent λ_{\max}) of q -twisted states, for a range of triadic coupling strengths σ_{Δ} . (c) Zoom-in view around $\lambda_{\max} = 0$ showing which twisted states are stable ($\lambda_{\max} < 0$). More twisted states become stable as σ_{Δ} is increased. (d) Fraction of twisted states that are stable as a function of σ_{Δ} , for $n = 83$ and $n = 830$.

II. RESULTS

A. Linear stability analysis

Here, we focus on an analytically tractable case of Eq. (1) equipped with a simple ring structure:

$$\begin{aligned} \dot{\theta}_i = & \frac{\sigma}{2r} \sum_{j=i-r}^{i+r} \sin(\theta_j - \theta_i) \\ & + \frac{\sigma_{\Delta}}{2r(2r-1)} \sum_{j=i-r}^{i+r} \sum_{k=i-r}^{i+r} \sin(\theta_j + \theta_k - 2\theta_i), \end{aligned} \quad (2)$$

where r is the coupling range. For the triadic coupling, we require $i \neq j \neq k$, so that each triangle involves three distinct nodes. Notice that we have set $\omega = 0$ by going into a rotating frame. Also note that we can always set $\sigma = 1$ by rescaling time, which we adopt throughout the rest of the paper. For demonstration purposes, all numerical results below are presented for Eq. (2) with $n = 83$ and $r = 2$, unless otherwise stated. The key findings remain qualitatively unchanged for other choices of the parameters.

Due to the rotational symmetry, twisted states are solutions to Eq. (2). We first show that triadic interactions can stabilize twisted states far beyond what is possible with pairwise coupling. To analyze the linear stability of any fixed-point solution $\boldsymbol{\theta}^*$ of Eq. (1), we can write down the Jacobian $\mathbf{J}(\boldsymbol{\theta}^*) = \mathbf{J}^{(1)}(\boldsymbol{\theta}^*) + \mathbf{J}^{(2)}(\boldsymbol{\theta}^*)$, where

$$\begin{aligned} J_{ij}^{(1)}(\boldsymbol{\theta}^*) &= \frac{\sigma}{k_i^{(1)}} A_{ij} \cos(\theta_j^* - \theta_i^*), \\ J_{ij}^{(2)}(\boldsymbol{\theta}^*) &= \frac{\sigma_{\Delta}}{k_i^{(2)}} \sum_{k=1}^n B_{ijk} \cos(\theta_j^* + \theta_k^* - 2\theta_i^*) \end{aligned} \quad (3)$$

for $i \neq j$ and $J_{ii}^{(\ell)} = -\sum_{j=1}^n J_{ij}^{(\ell)}$. For the rotationally symmetric topology considered in Eq. (2), the Jacobian

is a symmetric circulant matrix of the form

$$\mathbf{J} = \begin{bmatrix} J_0 & J_1 & J_2 & \cdots & J_2 & J_1 \\ J_1 & J_0 & J_1 & \cdots & J_3 & J_2 \\ \vdots & \vdots & \vdots & \ddots & \vdots & \vdots \\ J_1 & J_2 & J_3 & \cdots & J_1 & J_0 \end{bmatrix}. \quad (4)$$

We know that the normalized eigenvectors of a circulant matrix are the Fourier modes and the eigenvalues of \mathbf{J} are given by

$$\lambda_p(\mathbf{J}) = \sum_{s=0}^{n-1} J_s e^{2\pi i p s / n}, \quad 0 \leq p \leq n-1, \quad (5)$$

where $J_s = J_{n-s}$ for $\lfloor n/2 \rfloor < s < n$ [52]. This implies that λ_p are all real. Moreover, λ_0 is always equal to 0, and it represents the mode for which all oscillators are perturbed by the same amount. For any q -twisted state, $\boldsymbol{\theta}^{(q)}$, J_s is given by

$$\begin{aligned} J_s = & \frac{\sigma}{2r} \cos\left(\frac{2\pi q}{n}s\right) + \frac{\sigma_{\Delta}}{r(2r-1)} \sum_{k=-r}^r \cos\left(\frac{2\pi q}{n}(s+k)\right) \\ & - \frac{\sigma_{\Delta}}{r(2r-1)} \sum_{j=1}^2 \cos\left(\frac{2\pi q}{n}js\right) \text{ for } 0 < s \leq r, \end{aligned}$$

$$J_s = 0 \text{ for } s > r,$$

$$J_0 = -2 \sum_{s=1}^r J_s.$$

For example, for $r = 2$,

$$\begin{aligned} J_1 &= \frac{\sigma}{4} \cos\left(\frac{2\pi q}{n}\right) + \frac{\sigma_{\Delta}}{6} \left[1 + \cos\left(\frac{2\pi q}{n}\right) + \cos\left(\frac{6\pi q}{n}\right) \right], \\ J_2 &= \frac{\sigma}{4} \cos\left(\frac{4\pi q}{n}\right) + \frac{\sigma_{\Delta}}{6} \left[1 + \cos\left(\frac{2\pi q}{n}\right) + \cos\left(\frac{6\pi q}{n}\right) \right]. \end{aligned}$$

Plugging the formula for J_s into Eq. (5), we can analytically obtain the spectrum of the Jacobian for any q -twisted state and any coupling range r .

In Fig. 1(b)-(c), we show the linear stability of twisted states, measured by $\lambda_{\max} = \max\{\lambda_1, \lambda_2, \dots, \lambda_{n-1}\}$, as a function of the winding number q . We first note that the plot is symmetric with respect to $q = \frac{n}{2}$. This follows from the fact that twisted states with winding numbers q and $n - q$ are the same up to the reversal symmetry $\theta \rightarrow -\theta$ (the same symmetry applies to q and $-q$). Thus, below we will only consider $0 \leq q \leq \lfloor \frac{n}{2} \rfloor$. At $\sigma_\Delta = 0$, the stability curve has three peaks, and λ_{\max} becomes positive for $q > 11$. Thus, pairwise coupling in Eq. (2) cannot support stable twisted states with more than 11 twists (for $n = 83$ and $r = 2$). For systems with strong triadic couplings, the two side peaks are flattened while the central peak becomes more prominent. As a result, a lot more twisted states become stable. For example, all twisted states up to 33 twists are stable for $\sigma_\Delta = 4$. Interestingly, for intermediate σ_Δ , because λ_{\max} is a nonmonotonic function of q , winding numbers on disjoint intervals can become stabilized. For instance, at $\sigma_\Delta = 1$, twisted states are stable for $q \leq 14$, become unstable for $14 < q < 23$, then become stable again for $23 \leq q \leq 30$ (see Fig. 1(c) for details).

Figure 1(d) shows the fraction of stable twisted states P_{stable} as a function of σ_Δ , which further emphasizes the dramatic number of twisted states stabilized by triadic interactions. We see that P_{stable} is monotonically increasing with σ_Δ , and that one can easily go from less than 30% of stable twisted states to over 80% stable by adding triadic interactions. We also show the same curve for a larger system with $n = 830$, which is basically a smoother version of $n = 83$ (since there are a lot more twisted states for $n = 830$). Our results echo the recent findings in Ref. [53], which showed that higher-order interactions can stabilize twisted states in graphons.

B. Basin stability analysis

Next, we switch to the basin stability perspective. Figure 2 shows how the relative basin size p of the twisted states change with the triadic coupling strength σ_Δ . For $\sigma_\Delta = 0$, twisted states (including full synchrony), are the only stable states and thus take up the entire state space. States with fewer twists (smaller q) have a larger basin size. In particular, full synchrony attracts the most initial conditions. Now, for small σ_Δ , triadic interactions are affecting twisted states unequally: the basins for small q shrink whereas those for large q expand. As σ_Δ is further increased, the basins for the non-twisted states appear and quickly become dominant, whereas the basins of the twisted states all shrink and become comparable in size. Note that, among the twisted states, full synchrony does not have the largest basin anymore—in fact, the twisted state with the largest basin has more twists as σ_Δ is increased.

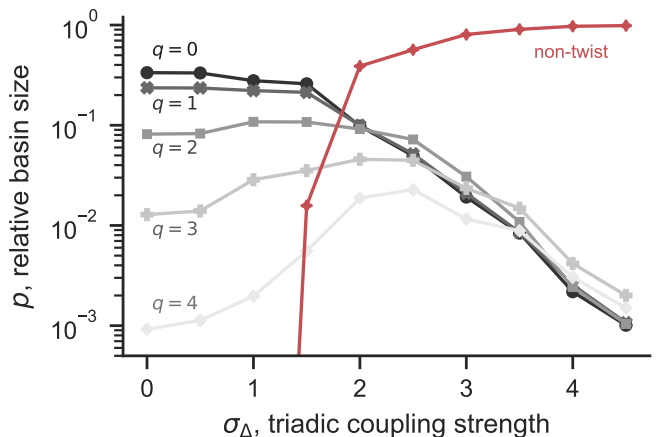


FIG. 2. **Higher-order interactions decrease the basin stability of twisted states.** We show p , the relative basin size, as a function of the triadic coupling strength σ_Δ . We estimated p by simulations starting from 10^5 random initial conditions. Each line represents a q -twisted state, except the red line, which represents attractors that are not twisted states. The relative basin size of non-twisted states quickly approaches 1 as σ_Δ is increased. We only show $q \geq 0$ due to the symmetry between q and $-q$.

Figure 3 further illustrates the opposite effects of higher-order interactions on linear stability and basin stability by visualizing the morphology of basins as σ_Δ is increased. Specifically, we examine a random 2D slice of the state space, spanned by $\theta_0 + \alpha_1 \mathbf{P}_1 + \alpha_2 \mathbf{P}_2$, $\alpha_i \in (-\pi, \pi]$. Here, \mathbf{P}_1 and \mathbf{P}_2 are n -dimensional binary orientation vectors in which $\lfloor n/2 \rfloor$ randomly selected components are 1 and the rest of the components are 0. We set the origin to be the twisted state with $q = 12$, $\theta_0 = \theta^{(12)}$, which we know from Fig. 1 is unstable when $\sigma_\Delta = 0$. Thus, we can only see basins for q between -3 and 7 in Fig. 3(a). Adding triadic interactions stabilizes $q = 12$, so we see its basin emerge in Fig. 3(b) when σ_Δ is set to 1. For larger σ_Δ shown in panels (c) and (d), the reduction in basin stability for twisted states becomes apparent. Despite their significantly improved linear stability, the basins for twisted states (as a group) rapidly shrink as more and more points get absorbed into the basin for non-twisted states (colored black), making twisted states hard to reach from random initial conditions.

The natural next question is: What are those non-twisted states created by higher-order interactions? Figure 4 shows that they consist of chimera states with increasingly large disordered domains as triadic couplings become stronger. Here, P_{order} measures the portion of oscillators that are ordered. Twisted states correspond to $P_{\text{order}} = 1$ and disordered states correspond to $P_{\text{order}} \approx 0$, whereas chimera states have P_{order} between 0 and 1. For final states reached from random initial conditions, the average P_{order} decreases from 1 to 0 as σ_Δ is increased.

We classify oscillators as (dis)ordered by calculating

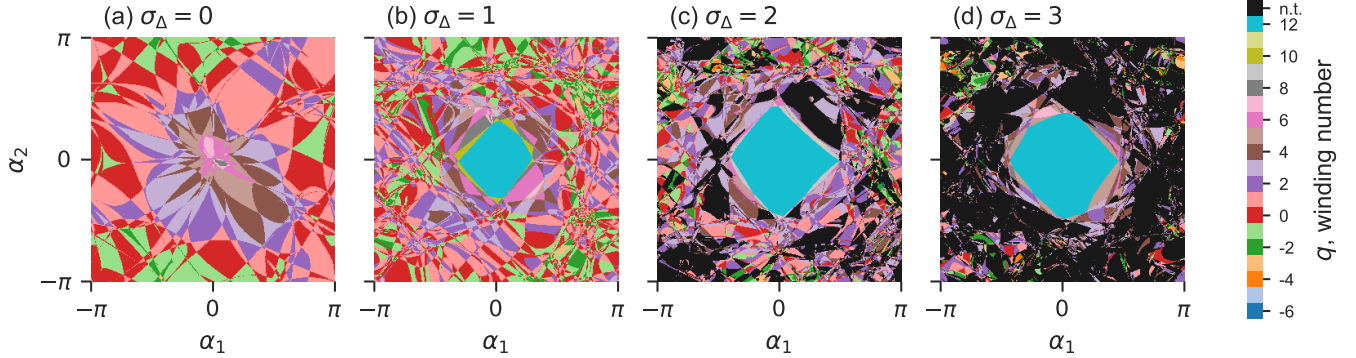


FIG. 3. **Higher-order interactions stabilize twisted states but shrink their basins.** Two-dimensional slices of the state space (centered around the twisted state with $q = 12$) showing how basins change as σ_Δ is increased. The basins of the twisted states are colored according to their winding number q , and the basins of all other states are colored black. (a) For $\sigma_\Delta = 0$, the twisted state with $q = 12$ is unstable, and all points converge to a twisted state with a lower winding number. (b) For $\sigma_\Delta = 1$, all attractors are still twisted states. Moreover, $q = 12$ becomes stable, which creates the cyan basin at the center. (c, d) For stronger triadic interactions ($\sigma_\Delta = 2$ and 3), the $q = 12$ basin expands, but non-twisted states also start to appear and quickly become dominant. Although the basin for $q = 12$ looks significant on the 2D slices, due to the high-dimensional nature of the state space, it would be almost impossible to reach from random initial conditions.

the local order parameters

$$O_j = \frac{1}{2r+1} \sum_{k=j-r}^{j+r} e^{i\theta_k}, \quad (6)$$

for $j = 1, \dots, n$. We classify oscillator j as disordered if $|O_j| < 0.85$. Other threshold values result in similar curves. The value of 0.85 is large enough to ensure $P_{\text{order}} \simeq 0$ for large σ_Δ , which matches visual inspection of the states.

The insets show typical attractors for different values of σ_Δ . Despite the fact that more and more twisted states become linearly stable for larger σ_Δ , they are increasingly unlikely to be observed from random initial conditions. Instead, the state space is dominated by the basins for chimera states (intermediate σ_Δ) or disordered states (large σ_Δ). This is consistent with recent results showing that higher-order interactions promote chimera states in simplicial complexes [54]. We note that the exact appearance of chimeras or disordered states can vary for different coupling ranges or coupling structures. However, the order-chimera-disorder transition described here is a robust phenomenon.

C. Other coupling structures

The above results for $r = 2$ remain qualitatively unchanged for other coupling ranges r . Figure 5 shows the opposite behavior of linear and basin stability for a wide range of r . For $r = 1$, 50% of the twisted states are stable under purely pairwise coupling. As σ_Δ is increased, all twisted states quickly become stabilized. As the coupling structure becomes more nonlocal (larger r), fewer twisted states are stable at $\sigma_\Delta = 0$. By introducing triadic couplings, one can always have at least twice as many stable

twisted states. For $r \geq 3$, we also observed the appearance of 2-cluster states, that is, with oscillators split (unequally) into two π -separated clusters (described, e.g., in [55, 56]), as shown in Figs. S1 and S2.

Aside from the generalization of Kuramoto models introduced in Eq. (2), there are several other natural ways to introduce triadic interactions. For example, we can turn the (pairwise) ring network into a simplicial (flag) complex by filling all pairwise triangles. This implies that $B_{ijk} = 1$ if and only if $i \neq j \neq k$, and all three pairs are within distance r : $|(i-j) \bmod n| \leq r, |(i-k)$

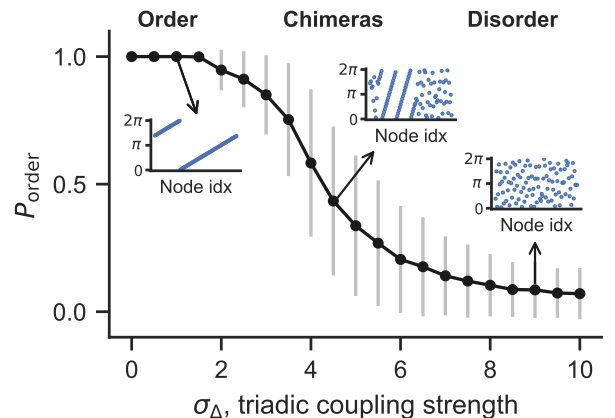


FIG. 4. **Chimeras bridge the transition from order to disorder as triadic interactions become stronger.** As we increase σ_Δ , we have a smooth transition from order (twisted states) to chimeras, and then to disorder. We monitor the transition by computing the portion of ordered oscillators P_{order} in the final state, averaged over 1000 simulations from random initial conditions for each σ_Δ . The error bars represent standard deviations and the insets show typical attractors reached from random initial conditions.

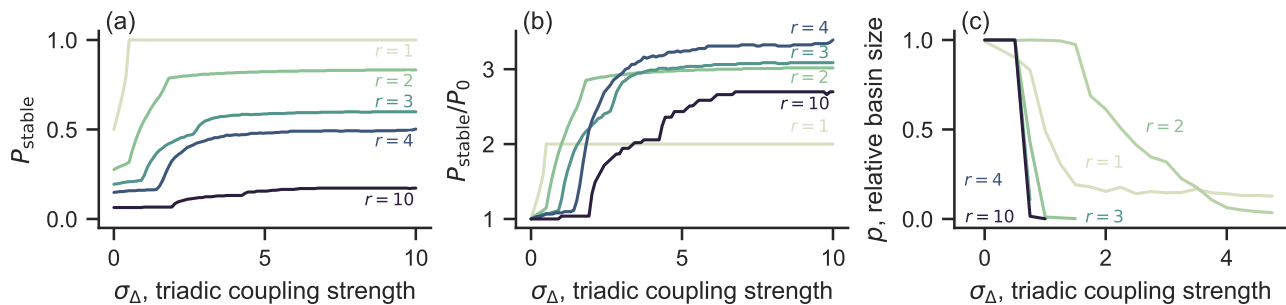


FIG. 5. **Higher-order interactions increase linear stability while decreasing basin stability for hypergraph rings with different coupling ranges.** (a) Fraction of twisted states that are stable as a function of σ_{Δ} , calculated with $n = 830$. (b) Same data as in (a), but shown as the ratio between the number of stable twisted states at nonzero σ_{Δ} and $\sigma_{\Delta} = 0$. (c) Relative basin size of all twisted states combined as a function of σ_{Δ} . For any given r , twisted states become more difficult to find as the triadic couplings become stronger. The basin sizes are estimated by simulating $n = 83$ oscillators from 10^3 random initial conditions.

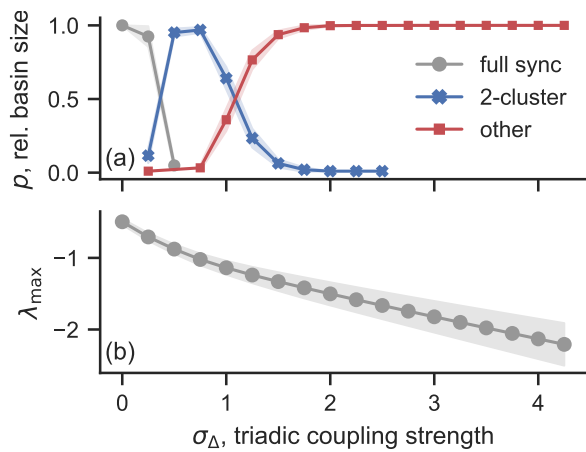


FIG. 6. **Synchronization becomes linearly more stable but harder to reach in random hypergraphs.** We show (a) the relative basin size of full synchrony (0-twisted), 2-cluster, and other (non-twisted) states, and (b) the maximum Lyapunov exponent for full synchrony. Results show the average over 20 random hypergraph realizations (with 100 initial conditions each). The shaded areas indicate one standard deviation.

$\text{mod } n| \leq r$, and $|(j - k) \text{ mod } n| \leq r$. In other words, $B_{ijk} = A_{ij}A_{ik}A_{jk}$. In comparison, the topologies considered in Eq. (2) do not require $|(j - k) \text{ mod } n| \leq r$ for $B_{ijk} = 1$. This can be expressed equivalently as $B_{ijk} = A_{ij}A_{ik}$. As shown in Fig. S3, the main results presented above for ring hypergraphs remain valid for simplicial complexes.

Finally, we demonstrate that a similar phenomenon persists in more irregular structures using random hypergraphs. There, the only twisted state that can be an attractor is full synchrony ($q = 0$). Similar to what we found above for more regular structures, in random hypergraphs triadic interactions make full synchrony linearly more stable [22, 31] but its basin of attraction shrinks dramatically in favor of 2-cluster states—for σ_{Δ}

up to around 1.5—and then more disordered states for stronger triadic coupling strengths (Fig. 6).

III. DISCUSSION

In this paper, we showed that higher-order interactions can make basins deeper but smaller—attractions become linearly more stable but at the same time are harder to find due to their basins shrinking dramatically. We demonstrated this phenomenon for Kuramoto dynamics with a wide range of coupling structures (ring hypergraphs with different coupling ranges, ring simplicial complexes, and random hypergraphs). We were able to characterize the linear stability of all twisted states analytically under these coupling structures. For basin stability, our systematic numerical simulations revealed interesting global features of the dynamics as σ_{Δ} is increased. In particular, the basins of twisted states become deeper but smaller due to the proliferation of new attracting states. We further characterized these new states introduced by higher-order interactions that compete with twisted states, which manifest as 2-cluster, chimera, or disordered states depending on the ratio between σ and σ_{Δ} .

Deeper but smaller basins induced by higher-order interactions can confer functional advantages to some biological systems. For instance, for the brain to function optimally [57], the attractors should have high linear stability so the brain can quickly return to the current state when subject to small perturbations or noise. At the same time, we also want the brain to be nimble and able to transition among different states efficiently (e.g., during computation and information processing), which can be achieved by having small basins.

Why do the basins of twisted states shrink as higher-order couplings are introduced? First, we note that, unlike their pairwise counterparts, Kuramoto systems with nonpairwise interactions are generally not gradient systems [58]. This provides the freedom for Eqs. (1) and (2)

to undergo Hopf bifurcations as σ_Δ is increased. Reference [59] showed recently that anti-correlation between linear stability and basin stability often emerges for dynamical systems that undergo consecutive Hopf bifurcations, offering a potential mechanism for higher-order interactions to shrink basins. More generally, as more attractors are created, the average basin size would decrease. In our case, the new states that emerge are more disordered than twisted states and they hold enormous entropic advantages (there are many more possible disordered configurations than ordered ones). Even 2-cluster states, which appear ordered on the surface, have many more configurations than twisted states—the oscillators can be divided between the two clusters in 2^n different ways [55].

Does extensive multistability emerge naturally from generic higher-order interactions regardless of details about the dynamics and couplings? Such phenomena have been observed under many different settings [54, 55, 60, 61]. For Eq. (1) with all-to-all coupling, it was shown previously that the coupling function $\sin(\theta_j + \theta_k - 2\theta_i)$ introduces a higher-order harmonic and nonlinear depen-

dence on the order parameter in the mean-field description, which create additional nonlinearity and extensive multistability in the self-consistent equations for the order parameters [62, 63]. The same is true for a different coupling function, $\sin(2\theta_j - \theta_k - \theta_i)$: Using the Ott-Antonsen ansatz [64], it was found that higher-order interactions give rise to added nonlinearity in the reduced equations that describe the macroscopic system dynamics [65]. Finally, for more nonlocal couplings, such as the ones considered here, we expect the nontrivial coupling structure could introduce additional nonlinearity into the macroscopic equations, further increasing multistability.

In conclusion, the prevalence of anti-correlation between linear stability and basin stability warrants a more nuanced and comprehensive approach when considering collective dynamics on hypergraphs and simplicial complexes. Understanding the global organization of attractors and saddles in the presence of nonpairwise couplings is crucial to the prediction and control of complex systems such as ecological communities and neuronal populations. We hope this work will stimulate future endeavors to understand the effects of higher-order interactions from both local and global perspectives.

-
- [1] R. Lambiotte, M. Rosvall, and I. Scholtes, From networks to optimal higher-order models of complex systems, *Nat. Phys.* **15**, 313 (2019).
- [2] F. Battiston, G. Cencetti, I. Iacopini, V. Latora, M. Lucas, A. Patania, J.-G. Young, and G. Petri, Networks beyond pairwise interactions: Structure and dynamics, *Phys. Rep.* **874**, 1 (2020).
- [3] L. Torres, A. S. Blevins, D. Bassett, and T. Eliassi-Rad, The why, how, and when of representations for complex systems, *SIAM Rev.* **63**, 435 (2021).
- [4] F. Battiston, E. Amico, A. Barrat, G. Bianconi, G. Ferraz de Arruda, B. Franceschiello, I. Iacopini, S. Kéfi, V. Latora, Y. Moreno, M. M. Murray, T. P. Peixoto, F. Vaccarino, and G. Petri, The physics of higher-order interactions in complex systems, *Nat. Phys.* **17**, 1093 (2021).
- [5] C. Bick, E. Gross, H. A. Harrington, and M. T. Schaub, What are higher-order networks?, *SIAM Rev.* **65**, 686 (2023).
- [6] F. Battiston and G. Petri, *Higher-Order Systems* (Springer, 2022).
- [7] I. Iacopini, G. Petri, A. Barrat, and V. Latora, Simplicial models of social contagion, *Nat. Commun.* **10**, 2485 (2019).
- [8] M. T. Schaub, A. R. Benson, P. Horn, G. Lippner, and A. Jadbabaie, Random walks on simplicial complexes and the normalized Hodge 1-Laplacian, *SIAM Rev.* **62**, 353 (2020).
- [9] M. Lucas, I. Iacopini, T. Robiglio, A. Barrat, and G. Petri, Simplicially driven simple contagion, *Phys. Rev. Res.* **5**, 013201 (2023).
- [10] N. W. Landry and J. G. Restrepo, The effect of heterogeneity on hypergraph contagion models, *Chaos* **30**, 103117 (2020).
- [11] G. St-Onge, H. Sun, A. Allard, L. Hébert-Dufresne, and G. Bianconi, Universal nonlinear infection kernel from heterogeneous exposure on higher-order networks, *Phys. Rev. Lett.* **127**, 158301 (2021).
- [12] U. Alvarez-Rodriguez, F. Battiston, G. F. de Arruda, Y. Moreno, M. Perc, and V. Latora, Evolutionary dynamics of higher-order interactions in social networks, *Nat. Hum. Behav.* **5**, 586 (2021).
- [13] G. Petri, P. Expert, F. Turkheimer, R. Carhart-Harris, D. Nutt, P. J. Hellyer, and F. Vaccarino, Homological scaffolds of brain functional networks, *J. R. Soc. Interface* **11**, 20140873 (2014).
- [14] C. Giusti, R. Ghrist, and D. S. Bassett, Two’s company, three (or more) is a simplex: Algebraic-topological tools for understanding higher-order structure in neural data, *J Comput Neurosci.* **41**, 1 (2016).
- [15] F. Parastesh, M. Mehrabbeik, K. Rajagopal, S. Jafari, and M. Perc, Synchronization in Hindmarsh–Rose neurons subject to higher-order interactions, *Chaos* **32**, 013125 (2022).
- [16] A. Santoro, F. Battiston, G. Petri, and E. Amico, Higher-order organization of multivariate time series, *Nat. Phys.* **19**, 221 (2023).
- [17] I. León and D. Pazó, Phase reduction beyond the first order: The case of the mean-field complex Ginzburg-Landau equation, *Phys. Rev. E* **100**, 012211 (2019).
- [18] M. H. Matheny, J. Emenheiser, W. Fon, A. Chapman, A. Salova, M. Rohden, J. Li, M. Hudoba de Badyn, M. Pósfai, L. Duenas-Osorio, *et al.*, Exotic states in a simple network of nanoelectromechanical oscillators, *Science* **363**, eaav7932 (2019).
- [19] E. Gengel, E. Teichmann, M. Rosenblum, and A. Pikovsky, High-order phase reduction for coupled oscillators, *J. phys. Complex* **2**, 015005 (2020).
- [20] I. Topal and D. Eroglu, Reconstructing network dynam-

- ics of coupled discrete chaotic units from data, *Phys. Rev. Lett.* **130**, 117401 (2023).
- [21] I. León, R. Muolo, S. Hata, and H. Nakao, Higher-order interactions induce anomalous transitions to synchrony, *Chaos* **34**, 013105 (2024).
- [22] M. Lucas, G. Cencetti, and F. Battiston, Multiorder Laplacian for synchronization in higher-order networks, *Phys. Rev. Res.* **2**, 033410 (2020).
- [23] A. P. Millán, J. J. Torres, and G. Bianconi, Explosive Higher-Order Kuramoto Dynamics on Simplicial Complexes, *Phys. Rev. Lett.* **124**, 218301 (2020).
- [24] L. Neuhäuser, A. Mellor, and R. Lambiotte, Multibody interactions and nonlinear consensus dynamics on networked systems, *Phys. Rev. E* **101**, 032310 (2020).
- [25] P. S. Skardal, L. Arola-Fernández, D. Taylor, and A. Arenas, Higher-order interactions can better optimize network synchronization, *Phys. Rev. Res.* **3**, 043193 (2021).
- [26] Y. Zhang, V. Latora, and A. E. Motter, Unified treatment of synchronization patterns in generalized networks with higher-order, multilayer, and temporal interactions, *Commun. Phys.* **4**, 195 (2021).
- [27] A. Salova and R. M. D'Souza, Cluster synchronization on hypergraphs, arXiv:2101.05464 (2021).
- [28] G. Ferraz de Arruda, M. Tizzani, and Y. Moreno, Phase transitions and stability of dynamical processes on hypergraphs, *Commun. Phys.* **4**, 24 (2021).
- [29] L. V. Gambuzza, F. Di Patti, L. Gallo, S. Lepri, M. Romance, R. Criado, M. Frasca, V. Latora, and S. Boccaletti, Stability of synchronization in simplicial complexes, *Nat. Commun.* **12**, 1255 (2021).
- [30] L. Gallo, R. Muolo, L. V. Gambuzza, V. Latora, M. Frasca, and T. Carletti, Synchronization induced by directed higher-order interactions, *Commun. Phys.* **5**, 263 (2022).
- [31] Y. Zhang, M. Lucas, and F. Battiston, Higher-order interactions shape collective dynamics differently in hypergraphs and simplicial complexes, *Nat. Commun.* **14**, 1605 (2023).
- [32] T. Carletti, L. Giambagli, and G. Bianconi, Global Topological Synchronization on Simplicial and Cell Complexes, *Phys. Rev. Lett.* **130**, 187401 (2023).
- [33] M. Nurisso, A. Arnaudon, M. Lucas, R. L. Peach, P. Expert, F. Vaccarino, and G. Petri, A unified framework for Simplicial Kuramoto models, arXiv:2305.17977 (2023).
- [34] P. J. Menck, J. Heitzig, N. Marwan, and J. Kurths, How basin stability complements the linear-stability paradigm, *Nat. Phys.* **9**, 89 (2013).
- [35] J. Milnor, On the concept of attractor, *Commun. Math.* **99**, 177 (1985).
- [36] E. Ott, *Chaos in dynamical systems* (Cambridge university press, 2002).
- [37] J. Aguirre, R. L. Viana, and M. A. Sanjuán, Fractal structures in nonlinear dynamics, *Rev. Mod. Phys.* **81**, 333 (2009).
- [38] P. J. Menck, J. Heitzig, J. Kurths, and H. Joachim Schellnhuber, How dead ends undermine power grid stability, *Nat. Commun.* **5**, 3969 (2014).
- [39] Y. Zhang, Z. G. Nicolaou, J. D. Hart, R. Roy, and A. E. Motter, Critical switching in globally attractive chimeras, *Phys. Rev. X* **10**, 011044 (2020).
- [40] S. H. Strogatz, From Kuramoto to Crawford: Exploring the onset of synchronization in populations of coupled oscillators, *Physica D* **143**, 1 (2000).
- [41] A. Townsend, M. Stillman, and S. H. Strogatz, Dense networks that do not synchronize and sparse ones that do, *Chaos* **30**, 083142 (2020).
- [42] M. Kassabov, S. H. Strogatz, and A. Townsend, Sufficiently dense Kuramoto networks are globally synchronizing, *Chaos* **31**, 073135 (2021).
- [43] M. Kassabov, S. H. Strogatz, and A. Townsend, A global synchronization theorem for oscillators on a random graph, *Chaos* **32**, 093119 (2022).
- [44] P. Abdalla, A. S. Bandeira, M. Kassabov, V. Souza, S. H. Strogatz, and A. Townsend, Expander graphs are globally synchronising, arXiv:2210.12788 (2022).
- [45] D. A. Wiley, S. H. Strogatz, and M. Girvan, The size of the sync basin, *Chaos* **16**, 015103 (2006).
- [46] R. Delabays, T. Coletta, and P. Jacquod, Multistability of phase-locking and topological winding numbers in locally coupled Kuramoto models on single-loop networks, *J. Math. Phys.* **57**, 032701 (2016).
- [47] D. Manik, M. Timme, and D. Witthaut, Cycle flows and multistability in oscillatory networks, *Chaos* **27**, 083123 (2017).
- [48] R. Delabays, M. Tyloo, and P. Jacquod, The size of the sync basin revisited, *Chaos* **27**, 103109 (2017).
- [49] Y. Zhang and S. H. Strogatz, Basins with tentacles, *Phys. Rev. Lett.* **127**, 194101 (2021).
- [50] S. Ashwin, J. Blawdziewicz, C. S. O'Hern, and M. D. Shattuck, Calculations of the structure of basin volumes for mechanically stable packings, *Phys. Rev. E* **85**, 061307 (2012).
- [51] S. Martiniani, K. J. Schrenk, J. D. Stevenson, D. J. Wales, and D. Frenkel, Structural analysis of high-dimensional basins of attraction, *Phys. Rev. E* **94**, 031301 (2016).
- [52] P. J. Davis, *Circulant matrices*, Vol. 2 (Wiley New York, 1979).
- [53] C. Bick, T. Böhle, and C. Kuehn, Phase oscillator networks with nonlocal higher-order interactions: Twisted states, stability, and bifurcations, *SIAM J. Appl. Dyn. Syst.* **22**, 1590 (2023).
- [54] S. Kundu and D. Ghosh, Higher-order interactions promote chimera states, *Phys. Rev. E* **105**, L042202 (2022).
- [55] P. S. Skardal and A. Arenas, Abrupt desynchronization and extensive multistability in globally coupled oscillator simplexes, *Phys. Rev. Lett.* **122**, 248301 (2019).
- [56] C. C. Gong and A. Pikovsky, Low-dimensional dynamics for higher-order harmonic, globally coupled phase-oscillator ensembles, *Phys. Rev. E* **100**, 062210 (2019).
- [57] M. Khona and I. R. Fiete, Attractor and integrator networks in the brain, *Nat. Rev. Neurosci.* **23**, 744 (2022).
- [58] C. Bick, T. Böhle, and O. E. Omel'chenko, Hopf bifurcations of twisted states in phase oscillators rings with nonpairwise higher-order interactions, arXiv:2310.15698 (2023).
- [59] P. C. Böttcher, B. Schäfer, S. Kettemann, C. Agert, and D. Witthaut, Local versus global stability in dynamical systems with consecutive hopf-bifurcations, *Phys. Rev. Research* **5**, 033139 (2023).
- [60] T. Tanaka and T. Aoyagi, Multistable attractors in a network of phase oscillators with three-body interactions, *Phys. Rev. Lett.* **106**, 224101 (2011).
- [61] P. S. Skardal, S. Adhikari, and J. G. Restrepo, Multistability in coupled oscillator systems with higher-order interactions and community structure, *Chaos* **33**, 023140 (2023).

- [62] C. Xu, X. Wang, and P. S. Skardal, Bifurcation analysis and structural stability of simplicial oscillator populations, *Phys. Rev. Res.* **2**, 023281 (2020).
- [63] C. Xu and P. S. Skardal, Spectrum of extensive multi-clusters in the kuramoto model with higher-order interactions, *Phys. Rev. Res.* **3**, 013013 (2021).
- [64] E. Ott and T. M. Antonsen, Low dimensional behavior of large systems of globally coupled oscillators, *Chaos* **18**, 037113 (2008).
- [65] P. S. Skardal and A. Arenas, Higher order interactions in complex networks of phase oscillators promote abrupt synchronization switching, *Commun. Phys.* **3**, 218 (2020).
- [66] N. W. Landry, M. Lucas, I. Iacopini, G. Petri, A. Schwarze, A. Patania, and L. Torres, XGI: A Python package for higher-order interaction networks, *J. Open Source Softw.* **8**, 5162 (2023).

Acknowledgements: We thank Melvyn Tyloo, Arkady Pikovsky, and Michael Rosenblum for insightful discussions.

Funding: YZ acknowledges support from the Omidyar Fellowship.

Author Contributions: YZ and ML designed the research. YZ, PSS, and ML performed analysis and simulations. All authors discussed the results. YZ and ML wrote the paper with feedback from PSS, FB, and GP.

Competing Interests: The authors declare that they have no competing interests.

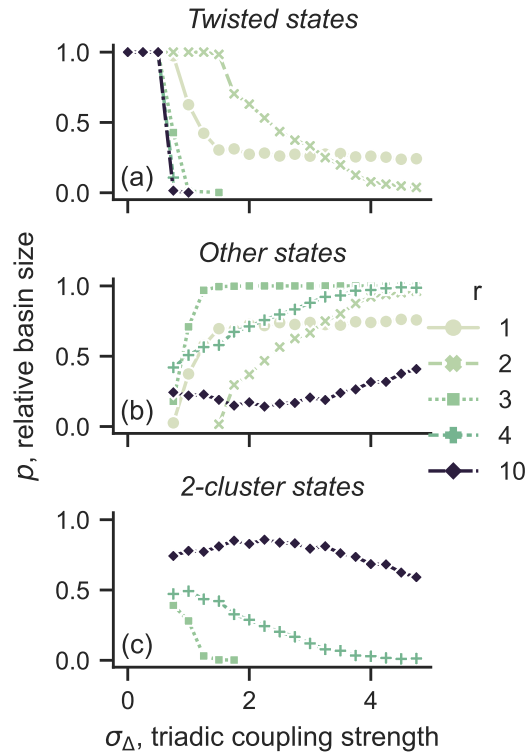
Data and materials availability: All data needed to evaluate the conclusions in the paper are present in the paper and/or the Supplementary Materials. Code for reproducing our results is available online from the repository https://github.com/maximelucas/basins_and_triangles. It utilizes the XGI package [66].

Supplementary Materials

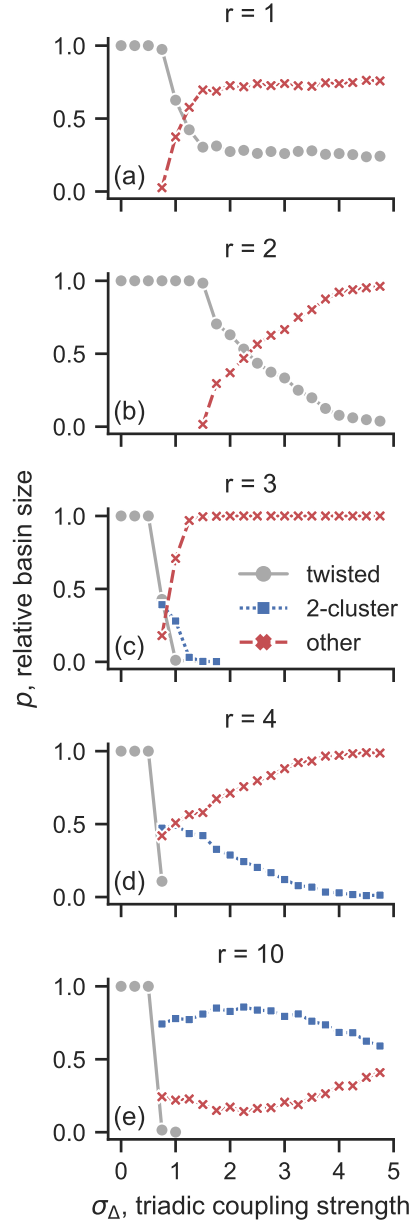
Deeper but smaller: Higher-order interactions increase linear stability but shrink basins

Yuanzhao Zhang, Per Sebastian Skardal, Federico Battiston, Giovanni Petri, and Maxime Lucas

S1. RING HYPERGRAPHS WITH DIFFERENT COUPLING RANGES



Supplementary Figure S1. **Extension of Fig. 5c for ring hypergraphs with different coupling ranges.** Here we also show relative basin sizes of 2-cluster states and other states. Two-cluster states appear for $r \geq 3$.



Supplementary Figure S2. **Same data as in Fig. S1 for ring hypergraphs with different coupling ranges.** Here we show the basin sizes per value of r .

S2. RING SIMPLICIAL COMPLEXES

For simplicial complexes, we consider systems described by the following equations:

$$\dot{\theta}_i = \frac{\sigma}{2r} \sum_{j=i-r}^{i+r} \sin(\theta_j - \theta_i) + \frac{\sigma_{\Delta}}{3r(r-1)} \sum_{\substack{0 < |k-i| \leq r \\ 0 < |j-i| \leq r \\ 0 < |j-k| \leq r}} \sin(\theta_j + \theta_k - 2\theta_i), \quad i = 1, \dots, n. \quad (\text{S1})$$

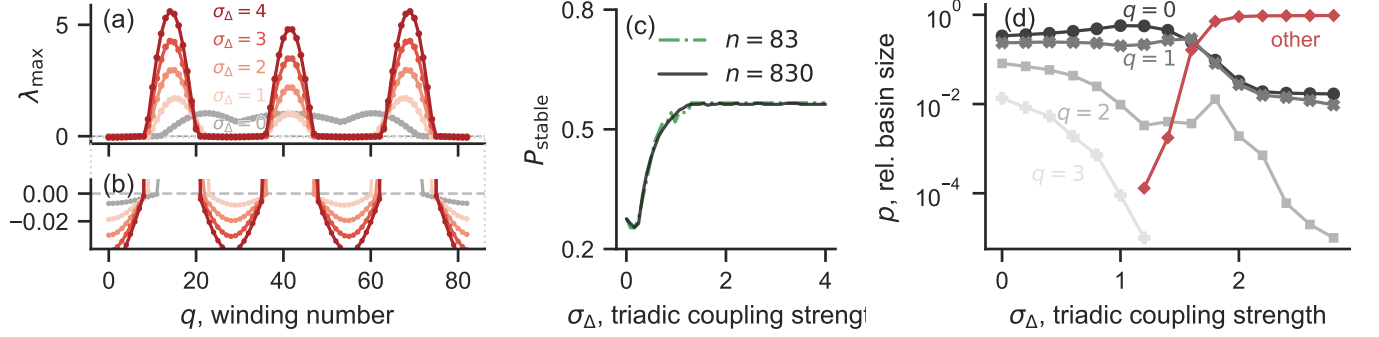
It is easy to verify that the coupling structure forms a simplicial complex for any coupling range r .

For simplicial complexes with coupling range r , we have

$$J_s = \frac{\sigma}{2r} \cos\left(\frac{2\pi q}{n}s\right) + \frac{2\sigma_\Delta}{3r(r-1)} \sum_{k=s-r}^r \cos\left(\frac{2\pi q}{n}(s+k)\right) - \frac{2\sigma_\Delta}{3r(r-1)} \sum_{j=1}^2 \cos\left(\frac{2\pi q}{n}js\right) \quad (\text{S2})$$

for $0 < s \leq r$. Specifically, for $r = 2$ we have

$$\begin{aligned} J_1 &= \frac{\sigma}{4} \cos\left(\frac{2\pi q}{n}\right) + \frac{\sigma_\Delta}{3} \left[1 + \cos\left(\frac{6\pi q}{n}\right)\right], \\ J_2 &= \frac{\sigma}{4} \cos\left(\frac{4\pi q}{n}\right) + \frac{\sigma_\Delta}{3} \cos\left(\frac{6\pi q}{n}\right). \end{aligned} \quad (\text{S3})$$



Supplementary Figure S3. **Analog of Figs. 1 and 2 for ring simplicial complexes.** Here, we show detailed results for the coupling range $r = 2$, but they remain qualitatively unchanged for larger r .